Mechanization of Rajiform Swimming Motion

The Making of Robo-Ray

University of British Columbia
Engineering Physics Project Laboratory
Applied Science 479 Final Report
Project Number 0159

Prepared for Dr. H. Davis
January 14, 2002

by
Renee Boileau
Lilian Fan
Tim Moore

Summary

This project is a preliminary step towards investigating the potential application of rajiform motion in underwater propulsion. In particular, a robotic model of one pectoral fin of the ray *G. micrura* has been constructed. This model is designed to mimic the swimming motion of the ray by using an actuated two-dimensional surface. The robot uses Shape Memory Alloy (SMA) wire as linear actuators to manipulate the fin surface in the manner of muscles. The actuator wires are controlled using a commercial interpreter software package running on a laptop computer. Swimming movements of the fish have been characterized to aid control algorithms. While certain desired shapes could be generated statically on the robotic fin, difficulties were encountered in actuating the fin dynamically due to problems in attaching the actuator wires. The model ray has been tested in a free-swimming mode at the BC Research Institute tow tank, but was unable to obtain self-propulsion. Despite this, indications of thrust were observed. Recommendations are made on the direction of continued work, including some design modifications.

Table of Contents

List of Figures

List of Tables

List of Equations

1 Scope

This report was prepared as part of the requirements for a senior student project in engineering physics at the University of British Columbia. This report contains the preliminary findings of the student project. For the most recent version, please contact the authors.

2 Introduction

This project was initiated to explore a method of fish locomotion as the basis for a possibly more efficient propulsion method. In particular, the project explores mimicking the swimming modes of rays, or "rajiform motion." Rajiform motion is arguably[1][*] one of the most efficient forms of fish locomotion, and is especially more efficient than conventional propulsion methods.

The objective of this project was to emulate the swimming modes of the ray *G. micrura*. Its scope includes: building a controllable two-dimensional surface capable of the shapes required for the straight-line swimming modes of rays and creating a control system for the surface based on a mathematical model of the swimming motions. The data for this mathematical model was taken from research done by L. Rosenberger[3] of the Field Museum of Natural History in Chicago.

This project is a preliminary step towards investigating the potential application of rajiform motion in underwater propulsion, and the primary goal for the project is to produce a first-generation robotic model of a ray fin. The robotic fin has been built and preliminary testing has been conducted. Shape Memory Alloy wires were used as an economical and simple actuator for the robot.

This report follows the design, construction and preliminary testing of the Robo-Ray robotic fin. It begins with an overview of the state-of-the-art in underwater motion research, followed by some background information on rajiform motion, details of the design and, finally, results and recommendations from testing the Robo-Ray. The design is broken down into the mechanical, electrical and control components.

[*] Numbers in square brackets [ ] indicate reference works listed in the References section at the end.

3 Background

Underwater locomotion is an energy-costly mode of transportation, since the drag of the entire vehicle must be overcome. Yet, ironically, underwater locomotion can be the least metabolically intensive way to get around the planet (see ref [1]). By making a vehicle neutrally buoyant, the effect of gravity can be neglected and the friction of the medium is the only effect that needs to be overcome.

However, artificial underwater locomotion is still often based on old surface transportation technology – the most common method of underwater propulsion being the propeller. Propellers are shielded in part by the body of the vessel, reducing their efficiency.

Other methods of underwater propulsion such as water jets have been developed. However, a new design methodology is taking the lead, based on successful living systems such as fish.

3.1 State-of-the-Art

Using designs based on fish swimming modes has proven to be a sound design method, having the benefit of millions of years of evolutionary design. Some projects currently being developed include MIT's Robotuna, based on thunniform motion (rear body flapping), and Penguinboat, based on rigid hydrofoil flapping. More in line with undulatory motion, a robotic lamprey is under development at Northeastern University, MA.

This project investigates a method of hydrofoil-driven motion called "rajiform motion," based on the swimming modes of ray fish. To our knowledge, there is no current bionics work on rajiform motion.

3.2 Rajiform Motion

Rajiform motion, which uses paired fins instead of whole body motion, has advantages in underwater propulsion design that include maintaining a rigid body for better sensory detection and better (even bi-directional) maneuverability [2].

Ray fish swim by using elongated, paired pectoral fins that have evolved to extend from opposite sides of a generally flat body. They use these fins to swim in a style called "rajiform motion," which includes two distinct modes.

The first mode is oscillatory motion, which is similar to bird flapping. Unlike most birds, however, the fin is not held as a rigid hydrofoil, but rather a standing wave pattern is created on the fin.

The second mode is undulatory motion. In this mode, a periodic waveform (a "ripple") travels along the fin from front to back, producing a net velocity aft.

Rajiform motion may include either mode exclusively or a combination of the two.

In the fish, the "bones" in the fin are actuated with two types of muscle – red fibre, which is aerobic, contracts slowly and can be used for long-duration swimming, and white fibre, which is anaerobic, less efficient, but better suited for short bursts of speed. In rays, the red fibre is intertwined with the white fibre, producing very smooth control.

Robo-Ray has only one type of "muscle fibre" – the SMA wire, which can be compared to red fibre, since it is relatively slow in response compared with the frequency of the motion.

Rays are swift, silent swimmers. These are desirable qualities in underwater vessels such as AUV's (Autonomous Underwater Vehicles) and ROV's (Remote Operated Vessels), enhancing their ability to perform environmentally sensitive missions such as wildlife observation, in addition to increasing their range. Rays also appear to be more efficient swimmers compared with fish which rely on other types of motion [3]. If a suitable technology

can be adapted to produce rajiform motion, a vessel using this motion for propulsion may also be more efficient.

3.3 Our Biological Ideal

Our project is based on a particular species of ray called *Gymnura micrura* or "smooth butterfly ray," pictured below in Figure 1.

Figure 1. Specimen of *G. micrura*

This species was chosen since it is known to use both types of rajiform motion and thus allows for a more general design that can be used to compare the two swimming modes. Key specifications for the *G. micrura* used in creating the scaled robotic model are shown in Table 1.

Table 1. *G. micrura* vs. model parameters

Variable	*G. micrura* [3] (mean)		Model
	non-dim	dim	
Scale factor, S_F	1		2.9
Disk Length, L_D		16.0 cm	46 cm
Disc width (root of fin), W_D		28.9 cm	-
Fin width, W_F		14.5 cm	42 cm
Fin beat frequency, f		1.29 Hz	1.29 Hz
Mid disc amplitude	0.20 (A/W_D)	5.8 cm	16.8 cm
Wave speed at 1/3 span	2.73 (c/L_D)		
Wave number	0.63 (L_D/λ)		
Stride length (U/f)		45.16 cm	
Phase velocity (U/c)	0.81		

4 Motion Analysis

The *G. micrura* produces motion that ranges from undulatory at low speeds to nearly pure oscillatory at high speeds. It does this by varying its wave number along the length of its body [3]. In order to design a robot that is a meaningful representation of this fish, the motion of the fish has been characterized and modeled mathematically.

While rajiform motion is complex and not fully understood, our robot can be adapted to perform a wide range of motions and the results compared to determine how these variations in wave number affect speed and efficiency.

The mathematical model was constructed based on the sequential photographs Rosenberger's paper [3]. Points in the photographs were tracked through the timed sequence and were then fitted to a series of curves. In order to fit these curves, this motion was originally modeled as a superposition of several gaussians. While this fit the photographic data well, it became apparent that the data is more intuitively described with a summation of sinusoids. The modelling material described in this report, then, will focus on these superimposed sinusoids.

4.1 Coordinate System

In order to describe dimensions and motion consistently with respect to both the fish and its robotic counterpart, it is necessary to introduce a coordinate system and define some important points. For underwater vehicles, the conventional arrangement for the Cartesian axes is as shown in Figure 2, with the x-axis parallel to the body, the y-axis perpendicular to the body and the z-axis pointing downward.

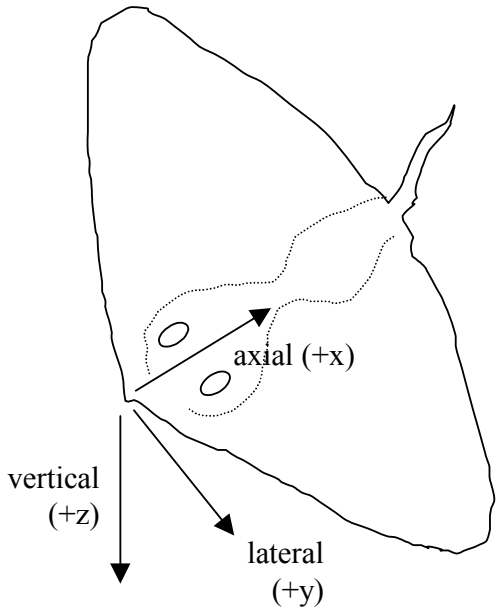

Figure 2. Coordinate axes and directions

It is useful to point out the regions for the fish shown in Figure 3 – where proximal is closest to the body, distal is away from the body; anterior is the front and posterior is the tail end, and dorsal and ventral are upper and lower surfaces, respectively.

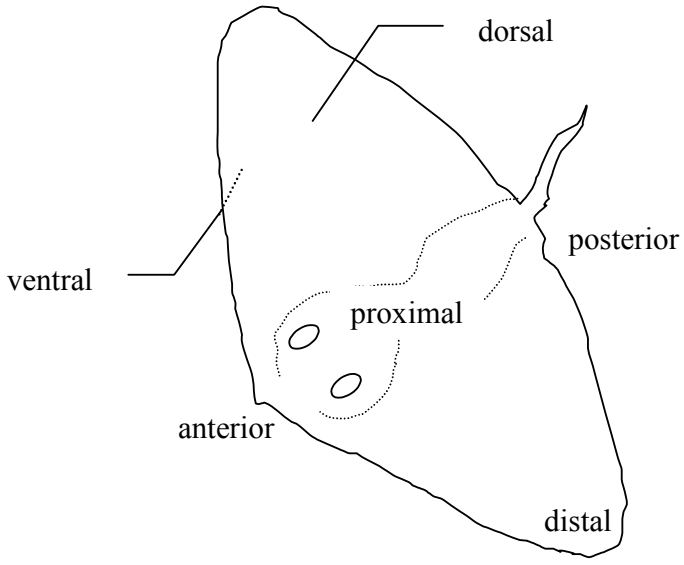

Figure 3. Region labels

4.2 Mathematical Model

The *G. micrura* motion is modeled as a combination of the fin shape, an oscillatory component and an undulatory component. The mathematical model has been based on the following relation:

$$Motion = C \cdot FinShape \cdot (UndulatoryComponent + OscillatoryComponent)$$

Equation 1. Mathematical model of *G. micrura* motion

where C is some constant, and the other terms are described below.

Fin Shape

The curve describing the outer (distal) edge of the fin at rest has been modeled by a generic sixth-order polynomial:

$$FinShape = -69.99x^6 + 207.08x^5 - 230.75x^4 + 117.09x^3 - 27.74x^2 + 4.41x - 0.01,$$

Equation 2. *G. micrura* fin shape

where x is the distance along the body of the ray (normalized to the length of the ray). The front (anterior) and the back (posterior) of the ray corresponds to x=0 and x=1 accordingly.

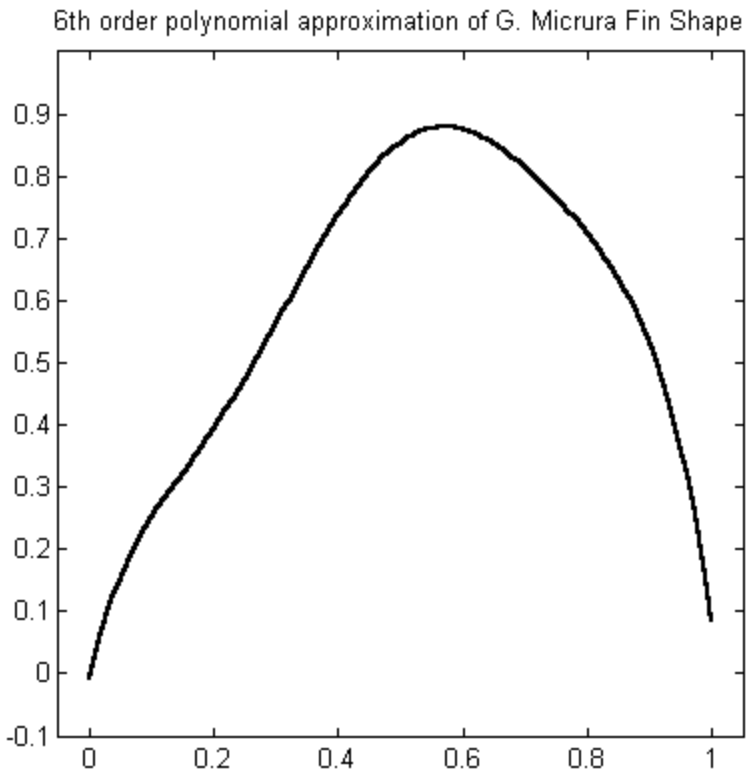

Figure 4. Fin shape approximation based on 6° polynomial

Undulatory Component

The undulatory component obtained from fitting the data is a periodic function represented by the following equations:

$$UndulatoryComponent = \sin\left(\frac{2\pi}{\lambda}(x-\phi)\right),$$
$$\lambda = 1.10 + 0.22\sin(8.40t + 3.64)$$
$$\phi = -0.03 + 1.41t$$

Equation 3. Undulatory component of *G. micrura* motion

where λ is the wavelength of the undulation and ϕ is the phase angle. These fits have been generated by the program IGOR Pro. They are valid over the range from 0 s to 0.74 s (period of oscillation of approximately 0.74s). The phase angle, representing the "characteristic ripple" along the ray's fin, appears to vary linearly with time. The wavelength of the undulation, on the

other hand, appears to be a periodic function of time. These relationships are graphically shown below, over a single stroke.

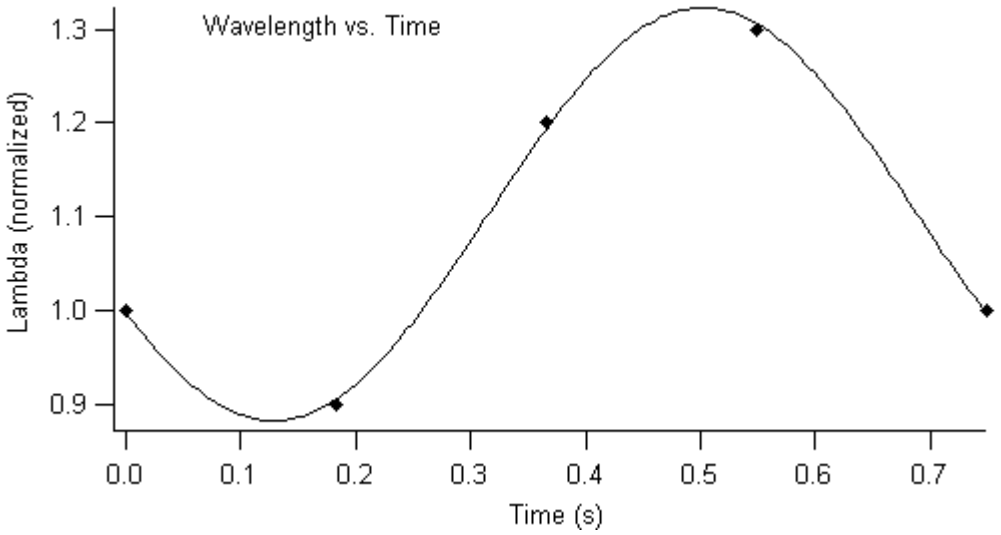

Figure 5. Change in wavelength as wave propagates along *G. micrura* fin

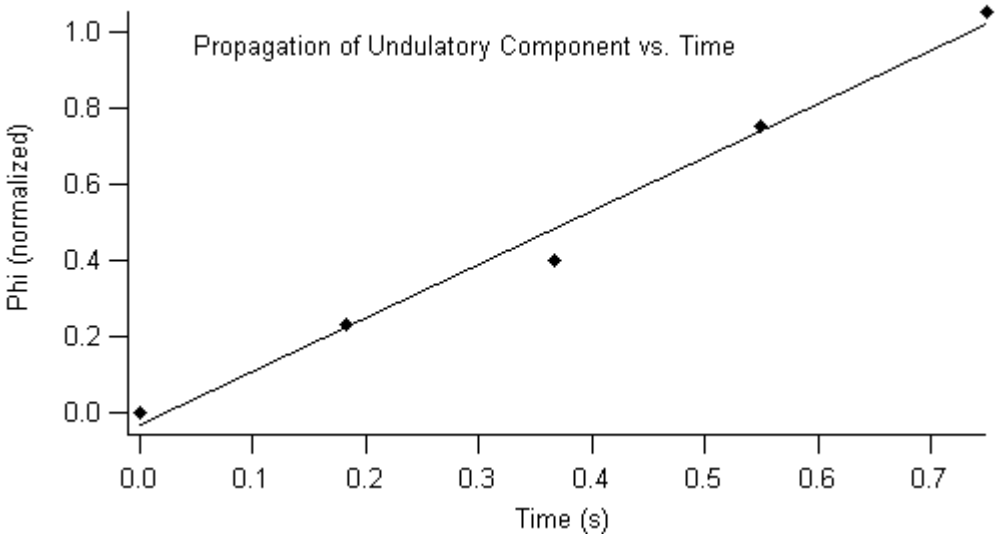

Figure 6. Propagation of undulatory wave component along *G. micrura* fin

Oscillatory Component

The oscillatory component of the fin motion also varies periodically over time. It is approximated by a sine curve in the model, although the fit for this parameter over time wasn't nearly as good as that of the other parameters.

$$OscillatoryComponent = 0.1 + 1.25\sin(8.5t)$$

Equation 4. Oscillatory component of *G. micrura* motion

The corresponding plot for the oscillatory component is shown in Figure 7.

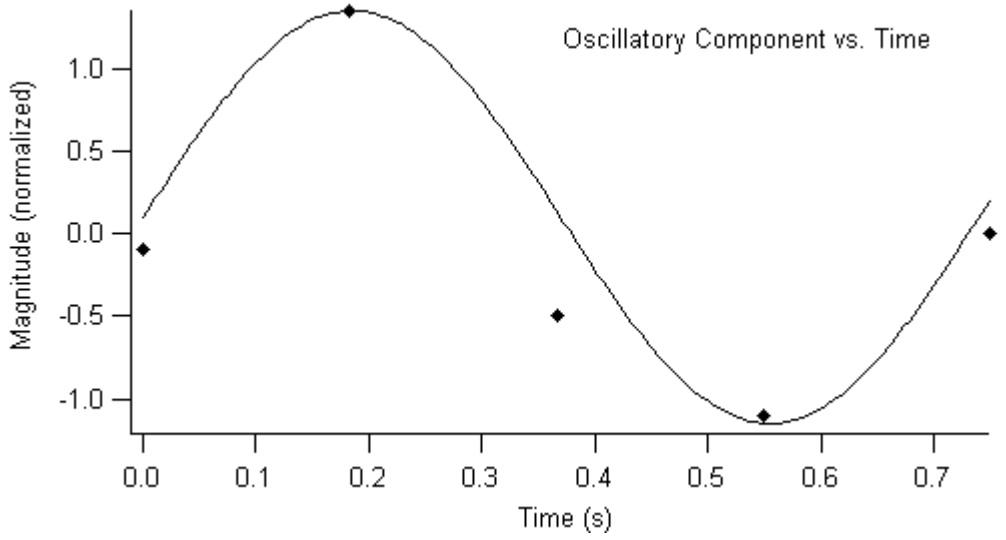

Figure 7. Amplitude of oscillatory wave component in *G. micrura*

Combined Motion

Curves that are relatively similar to the data obtained from the photographs were generated by combining the oscillatory and undulatory equations of motion as shown in Equation 1. These are plotted in Figure 8 along with the data from the photographs.

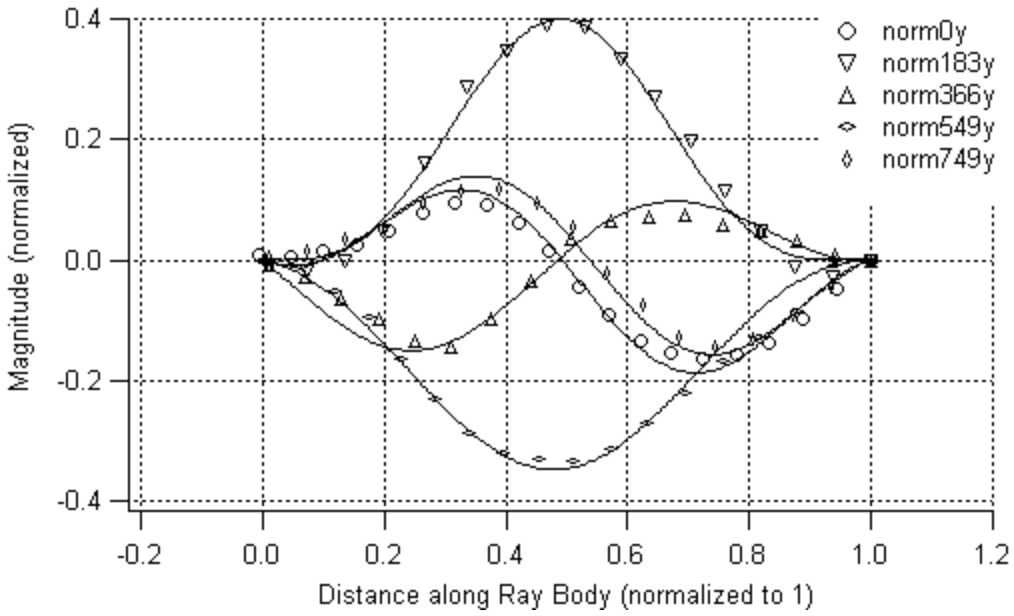

Figure 8. Mathematical model of *G. micrura* fin edge motion

The preceding plots show that the ray's motion can be described quite well as a combination of sinusoidal motions.

It has been observed in literature [4] that one method by which the *G. micrura* (along with several other batoid species) increases its swimming velocity is by decreasing significantly its wave number (i.e. increasing the wavelength). Our observation of the wavelength dependence over time (within a single stroke cycle) translates to having the minimum wavelength at the upstroke and a maximum wavelength coinciding with the downstroke. While this variation of the ray's wave number may simply be a statistical anomaly[†], it is certainly possible that it plays an important part the ray's general locomotion.

The phase of the travelling wave propagating along the length of the ray increases over time and represents intuitively the characteristic "ripple" of rays performing undulatory motions. The phase appears to fit nicely on a straight line save for one of the five data, where a value much less than that predicted by the linear fit was observed. This point occurs on the downstroke,

[†] We do, after all, only have data for one stroke cycle of the fish.

indicating that the ray may be producing more of its power on this part of the stroke. Such a concept has also been suggested by Hamlett [5].

Of interest to note is that for two of the time instances out of the five data, the wavelength of the ray also appears to increase along the length of the ray, however there is insufficient data in the photos we have to determine if that is indeed the case. Therefore, wavelength is treated as a function of time only in this model.

The errors for the data points shown in Figure 8 are approximately ±0.01 after normalization. Evidently some of the fits are not within error, but that was the best that could be done for the present time. More photographs of the swimming ray would help determine the validity of this approach.

5 Mechanical Design

The mechanical construction of the robot parallels the anatomical structure of one pectoral fin of *G. micrura*. It consists of four main elements: the sail membrane, corresponding to the surface of the fish fin; the actuator lines, corresponding to the muscles in the fish; the battens, which support and deform the sail like the cartilage in the fish; and the body, which corresponds to the body of the fish.[‡]

The sail provides the actuating surface. It also prevents rotation of the frame elements, or "battens," about the vertical axis. The sail is articulated by selectively applying a bending moment to each individual batten. The bending moment is applied to each batten by actuating one of a pair of actuator lines attached to the dorsal and ventral sides of each batten. The body of the prototype clamps the membrane and battens in place, provides the attachment and tensioning point for the actuating lines, and also houses and protects the electrical control system.

5.1 Assumptions

The robot is not identical in structure to the fish. The following assumptions were used when designing the mechanical fin:

- that the *G. micrura* has a symmetric swimming stroke, as suggested by photographs in the Rosenberger article [3]
- that since the motion is symmetric laterally, a single half-model should represent the fish accurately
- that a symmetric top and bottom of the ray body will be a reasonable approximation
- that since the body is symmetric, propulsion is also symmetric

[‡] Note: to avoid confusion between the fish and the robot, nautical terms are used here when describing the robot.

- that muscle elements would take on a parabolic shape in bending
- that the frame elements, or "battens," are a single continuous piece
- that the submerged elements of the fin are neutrally buoyant
- that the actuating muscle elements are all parallel

The last assumption was made after studying a preserved specimen at the UBC Fish Museum.

In spite of scaling the fish up by a factor of 2.9, size was critical in choosing the actuation system for the robot. The number of elements that must be actuated necessitates a small and inexpensive actuation system. A relatively new technology called Shape Memory Alloy (SMA) wire was chosen as a solution to both these criteria.

5.2 Muscle Wires

Simulation of muscular actuation was achieved using Shape Memory Alloy (SMA) wires. SMA is a metal alloy that undergoes a phase change at an actuation temperature which is a property of the material. SMA is ductile martensitic alloy below its actuation temperature and can be plastically deformed, but reverts to its original length and stiffness in an austenitic form after heating above this temperature. This material provides sufficient force for our model, makes a very compact actuator and is very economical.

SMA wire was found to be the most economical method of actuating the wires (compared with hydraulic and motor-driven systems, for example). Each linear actuator, having a stroke length of approximately 6 mm, cost in the neighbourhood of $10 per piece. This can be compared to approximately $100 dollars per piece for an actuated control valve required for a pneumatic system or approximately the same cost for servo motors. Hydraulic actuation would have been even more prohibitive. Complicated assemblies with integral feedback positioners and electric-to-pneumatic (IP) converters run from $1000 to $10,000. Of course, it may be possible to

produce a pneumatic or hydraulic system with home-made actuators, but this approach would have pushed the scope of this project far beyond the available time and resources.

SMA wire is also the most compact actuator we could find. Our model has 20 actuators packed into 114 cubic inches; each actuator takes up a space of only 1"x 1.5"x 3".

The SMA actuators are not without their difficulties. SMA wire exhibits a significant hysteresis in its mechanical properties during heating and cooling. The requirement of controlling the temperature of the wire in water makes the wire inefficient and difficult to control. The control difficulties are an artifact primarily in the sense that, while the heat input to the wire can be controlled, the cooling of the wire is dependent on factors not easily changed. These factors include the temperature of the surrounding water and the thermal resistance of the latex tube covering.

The latex tube covering is necessary since the wire must be electrically isolated. It is also necessary to ensure that the wire reaches its relatively high actuation temperature (70°C to 120°C). The latex tube acts as both a thermal and electric insulator.

In total, the fin has ten dorsal/ventral pairs of SMA wire, arranged to actuate the proximal two-thirds of the frame.

5.3 Battens

The frame of the robotic fin consists of eleven evenly spaced parallel cylindrical rods, or "battens," oriented perpendicular to the direction of motion. The battens are clamped in slots in the central body plate. (One batten is passive since there were not enough control lines from the computer.)

Each batten is fitted with a distal termination block (DTB) at a point two-thirds of the way from the body. The distal termination blocks are used to translate the force from the actuating lines into an applied moment on the batten.

Each actuator set consists of two SMA wires. One wire is doubled over and placed around the distal termination block to form the dorsal "muscle," and a second wire forms the ventral "muscle" in the same fashion on the opposite side of the batten. The latex tubes containing the actuator lines are looped over stacked washers screwed into the ends of the distal termination blocks. In addition, the battens are equipped with intermediate masts, designed to hold the wire to approximately the same curve as the batten, but not transmit any torque to the batten. Figure 9 shows the profile view of a single assembled batten (with the membrane removed for clarity).

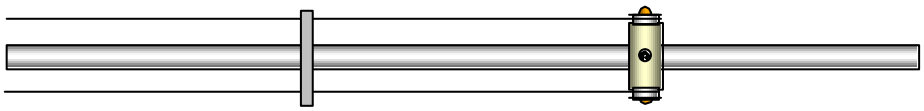

Figure 9. Profile view of batten assembly

One of the things that make using bionics a low-energy-cost system is the materials from which the system is built. The stiffness of the cartilage forming the skeleton of the fish helps store energy during each stroke and produces a restoring force that assists on the return stroke. Likewise, flexible polycarbonate (PC) rods were chosen for the battens. These PC rods are sufficiently stiff to prevent buckling, yet are elastic enough so that 10-mil SMA wires can bend the frame. Polycarbonate has superior elastomeric mechanical properties, is much stronger in compression and is less brittle than other plastics such as acrylic or Plexiglas. It was also chosen over metals since it is nearly neutrally buoyant in water (s.g. = 1.2). The battens are sized to extend to the edge of the fin shape. The latex rubber tubes containing the actuator lines are lashed to the frame with nylon whipping twine in the manner described in section 5.2.

Each DTB is threaded though the cylindrical axis (#4-40) to accept two machine screws. The screw secures a thick washer capped by a flat washer. This assembly acts as a bearing pint for the SMA wires. The installed assembly can be seen diagrammatically in Figure 9.

5.4 Intermediate Masts

To constrain the muscle wire to a curve that runs approximately parallel to the bone rod, the wire is attached to the bone at one or two (depending on the length of the wire) intermediate points. These attachment points are meant to provide a constraint on the wire to a fixed distance away from the bone, without constraining any side-to-side motion. To achieve this, the dorsal and ventral wire pairs were attached together though the fin membrane with a loop of string. A short length of rigid tubing between the bone and each wire maintained the separation from the bone.

This arrangement was a compromise solution adopted due to time constraints. For the tests in water, the lashing holding the wires together worked loose and allowed the relaxed muscle wire to collapse beside the bone. This proved to be a problem when the collapsed wire was re-actuated. Instead of inverting the curve of the bone, the re-actuated wire compressed the existing curve and producing an S shaped fin profile. This is shown schematically below in Figure 10. To make matters worse, after four or five of the bones had been actuated, one of the bones (typically one from the posterior region of the fin) would invert properly and "pop" the preceding elements over into the correct profile. This would send a very fast wave propagating in the wrong direction along the fin.

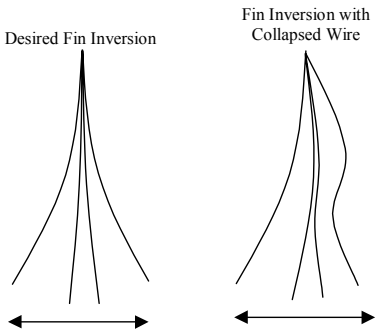

Figure 10. Bone inversion

Correct fin inversion, and therefore the intermediate attachment points, could prove to be the critical aspect to generating thrust by means of rajiform motion.

Finally, a system was designed so that the SMA wires could be tensioned manually to the desired amplitude.

5.5 Slide Tensioners

The SMA muscle wires were tensioned using slide tensioners. These tensioning devices consist of a plastic block, threaded though the long axis, with a rabbet cut across one end. The rabbet retains two sets of aluminium clamping blocks. The lower block is threaded and the blocks are positioned such that the clamp can be tightened from above with a machine screw. The ends of the SMA wire were placed between the clamping blocks and the screw tightened from above onto the electrical connection. This provides electrically isolated connections to each-end of the wire, one of which is connected to a common terminal V+, while the other connection is switched. The wires are tensioned using the ¼-inch screws threaded into the back of the block. The block's position can be adjusted over a range of approximately an inch to accommodate variations in the wire length after clamping and any pre-stretch given to the line during handling.

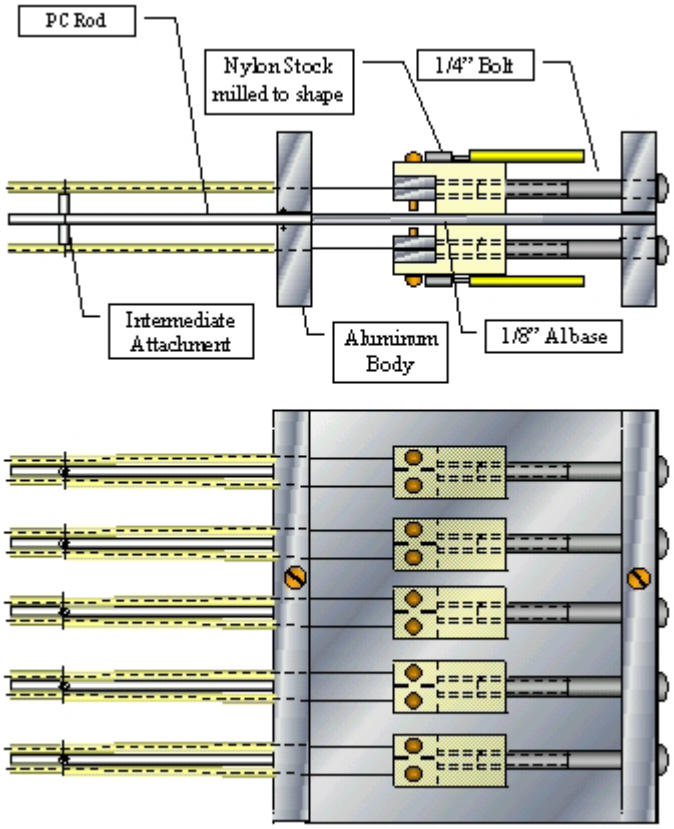

Figure 11. Slide tensioner assembly

5.6 Prototyping (a brief history)

Prior to building the robotic fin, several single element prototypes were built. The first of these was simply a sheet of polycarbonate with a wire attached to each side. The wires were pulled by hand to "flap" the prototype. This first prototype was used to demonstrate the concept of using actuating lines to create a curved surface on the fin. In looking at this first prototype, it was realised that the original intention of using a continuous sheet of polycarbonate as the fin surface would not work well, since different stiffnesses were needed perpendicular and parallel to the motion of the waveform to create a complex curve. To achieve this, the design was modified to create a framework of actuated elements (battens) and embed them in a rubber casing. To replace the continuous sheet of polycarbonate, 1/8-inch polycarbonate rods were chosen. These were

slipped into pockets in a 3/8” thick rubber sheet, made up by laminating three layers of rubber together.

A single element prototype of the new design was made. This prototype was fitted with a single muscle of SMA wire on one side. While experimenting with this prototype, however, it quickly became apparent that the rubber was far too stiff for the application. During the design phase, it was assumed that the rubber sheet would act as a membrane with no appreciable bending moment. However, this was not the case (a 3/8 x 1-inch strip of rubber is much stiffer than a 1/8-inch rod of polycarbonate). Since increasing the amount of force applied to the fin was not an attractive option, another way of providing the fin surface and attaching the wires needed to be found.

In the next generation of prototype, the rubber surface was replaced with a light (spinnaker weight) sailcloth. A photograph of this prototype is shown in Figure 12.

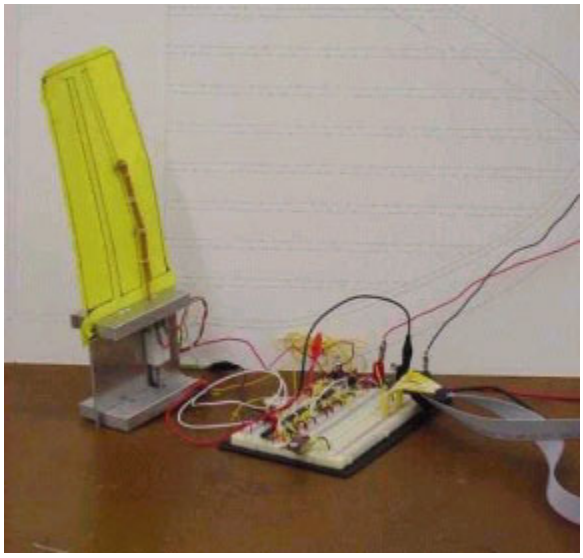

Figure 12. Prototype fin

Two layers of sailcloth were sewn together to provide pockets for the battens. The polycarbonate rods were inserted into the pockets and a distal termination block was placed on the rod through a hole in the cloth, at two-thirds of the distance from the body to the tip of the

rod. Initially a single element prototype was built, but proved to be too unstable, as the narrow strip of cloth could not constrain the motion of the batten to a flapping motion, but would allow the wires and batten to collapse sideways. To address this problem, a two-element prototype was built, and with the extra width the actuated element was properly constrained to a flapping motion. The next challenge was to devise a method to tension and adjust the muscle wires so that the amplitude of the fin could be controlled.

The original design idea for the tensioning involved the use of guitar string tuning devices. However, this had several drawbacks: expense (two to five dollars each, 20 required), difficulty in mounting, and lack of symmetry in tensioning. The lack of symmetry arose from the fact that only one side of the wire loop would be tensioned. This, depending on the friction of the wire around the distal termination block, could lead to half the SMA wire being in much greater tension than the other half. To address these problems, the slide tensioners used in the final model were designed.

To test the response of the prototype, a test circuit was designed to supply a periodic UP-OFF-DOWN-OFF signal to the actuated element of the prototype. The signals were given approximately equal time weight in the tests. Testing of the whole assembly consisted of mounting the new membrane and batten combination on a two-wire tensioning device (the slide tensioners at the body), which in turn was wired to the test circuit. The test circuit actuated only one wire at a time in alternating fashion and the response of the assembly was analysed. The analysis was carried out by taking a digital video of the element motion and plotting the position of the tip of the batten over time. A plot obtained from one such test is illustrated in Figure 13.

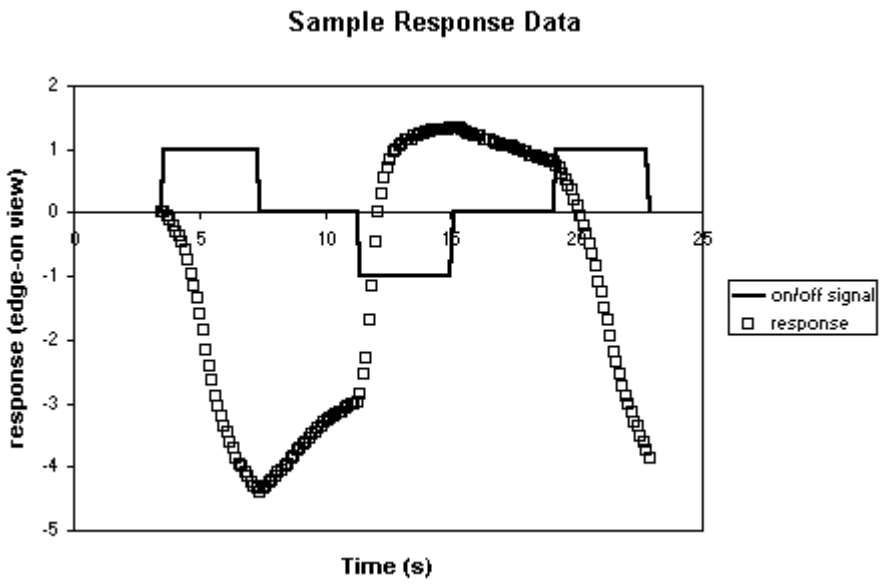

Figure 13. Response of filmed prototype

The up, down and off portions of the signal are depicted as 1, -1 and 0 on the plot to provide a reference point. The hysteresis in SMA wire can easily be seen on this plot. Results from subsequent movies (after some tuning of the prototype) show a more consistent response over time, and suggests possibilities of relatively good control of the SMA wires given a reasonably well-controlled environment.

The prototype model showed that this design allowed the prototype fin to easily obtain the required maximum amplitude. However, one problem that was never solved satisfactorily is the collapse of the intermediate attachment points. Several attempts were made to solve this problem, but none with great success (see section 5.4 on intermediate attachments)**.**

5.7 Muscle-Skeleton Interaction

To estimate the expected forces that the muscle elements will be required to apply, the bending moment required to bend the bone elements has been estimated. To simplify the calculation, the bending moment of the sailcloth membrane has been neglected in the moment calculation. Likewise, the forces applied to the bone by the intermediate attachment points were neglected as

these forces are presumably small. The second moment of inertia for each element of the skeleton is then calculated as

$$I = \frac{\pi D^4}{64},$$

where D is the diameter of the skeletal rod. The relation below gives the moment, M, required to bend the distal termination block of the muscle/skeleton to a given vertical displacement, y:

$$M = \frac{2EI}{x^2} y,$$

where x is the length of the bone, measured from the body to the distal termination block and E is the modulus of elasticity for polycarbonate. The passive end of the rod will continue the slope of the bone from the distal terminal block to come to the final amplitude of the fin at the tip.

The maximum required moment is characterized by the distance between the actuator wire and the neutral axis of the fin. The height of the distal termination blocks, the intermediate attachments and the body attachments of the SMA wires set this distance. For our prototype, this distance was kept constant, but need not have been. The 0.010" SMA wires used in the prototype are capable of providing a maximum pull of 1 kg (10 N) each. The doubled-over wire in the prototype can therefore transmit a total force of 20 N to the distal termination block. The force, F, required to create the moment required is given by

$$F = \frac{M}{d},$$

where d is the distance from the applied force to the neutral axis. The force required to bend the beam model statically to its maximum amplitude (y) is approximately 10 N. In addition to bending the skeleton, the actuated muscle must also stretch the opposite wires back to their extended length. To stretch the wires back to their extended form, the contracting muscle must

apply an additional 3 N of pull. This leaves approximately 7 N of force to provide the dynamic forces needed to move the water through the water.

6 Control Design

Any robotic device requires some means of control. In this project, a method of controlling twenty Shape Memory Alloy (SMA) actuators to mimic the undulatory and oscillatory motion of the *G. micrura* is required. In light of the fact that this is our group's preliminary attempt at analyzing and investigating the dynamics of such motions, not to mention the relatively unpredictable response behaviour of the SMA, it is important that a controller be designed and built in a way such that any modifications to the "programming" of the fin's motion can be easily and quickly facilitated.

Numerous options were considered at the early stages of the project. The primary candidates included open/closed loop control with a micro-controller/personal computer. The unique characteristics of SMA wire made designing feedback sensors a task beyond the scope of the current project, resource- and time-wise. In addition, the number of actuators that must be controlled rendered the option of using micro-controller boards far beyond this project's budget. Consideration must be given as well for the need to perform testing at a tow tank. As a result, a portable personal computer is used to control the robot without feedback.

Given that the SMA actuator response varies significantly depending on its exact material composition, load, mounting geometry, temperature and thermal history, it was deemed best to have an additional device built to test a two-wire (one actuated bone) prototype of the fin.

6.1 Hardware

Prototype Testing Circuit

The prototype test procedure consists of activating one actuator for about four seconds, then allowing it to rest for four seconds before the actuator on the opposite side of the prototype is actuated in similar fashion (refer to Figure 13 in section 5.6 for sample test results). Only one actuator turns on at any one time. A circuit using three 74HC4538 Dual Precision Monostable

Multivibrator chips was designed[§] and assembled to achieve this. The schematic of this test circuit is included in the appendices.

Controlling the Robot

As previously mentioned, portability is relatively important to ensure testing proceed as smoothly as possible. Thus, a laptop computer is used to control the robot through the computer's parallel port. An Advantech multipurpose I/O card (PCL-712) was set up during the course of the project as part of a contingency plan.

In turn, since the computer's parallel port has only eight lines of direct output[**], an external circuit that latches output from the parallel port was designed and built. A circuit diagram is included pursuant the following circuit description.

Latching Circuit

The latching circuit is the interface between the computer and the SMA actuators. Latches are needed to "store" data for 20 lines (20 actuators) since only eight lines can be updated by the parallel port at any one time. It may be useful to know that the components used in our project are chosen because they are readily available at the project lab.

The latching circuit consists of a 74LS139N Dual 1-of-4 decoder and four 74HC373AN Octal Transparent Latches. Several logic gates, a LM7805 voltage regulator and a 74LS244N octal buffer make up the rest of the circuit.

The Logistics of the circuit are as follows:

- All output lines from the parallel port (D0 to D7 – eight lines in all) are buffered[††] (using the 74LS244N Octal Buffer). Two of the buffered lines (D6 and D7) are used

[§] Many thanks to Al Cheuck for coming up with initial rough sketches of the design!
[**] There are four additional bi-directional lines in the parallel port that we did not wish to deal with
[††] A buffer is needed when a gate has to drive a relatively large fanout. (this isolates the load (the circuit) from the source (the parallel port))

for encoding, five lines (D0 to D4) are used to transmit data (instructions for the robot) and one (D5) is used as a flag to keep track of when the encoder lines are updated and when the data lines are updated.

- Data lines (D0 to D4) are shared by 4 Octal Transparent Latch chips (74HC373AN). The 74HC373AN consists of 8 transparent latches that share a common Latch Enable (LE). When LE is high, each of the eight outputs takes on the logic state of the corresponding input. When LE is low, the outputs are latched – that is, any changes to the inputs have no effect on the outputs. For each octal latch, only 5 of the latches are used. Each data line (D0 to D4) is connected to an input at each of the four Octal Latches.
- The two encoder-lines (D6 and D7) are decoded with a 74LS139 1-of-4 decoder. This decoder accepts two inputs and provides four active-low outputs[‡‡]. This way, one of the four latches may be selected for updating at any one time using the two encoder-lines.
- The four decoded lines are then inverted and passed onto one of the inputs of a 2-input AND gate.
- The buffered flag D5[§§] is used to indicate when the encoder lines are being updated (when D5 is logic low), and when the outputs of the Octal Latches are being refreshed by the information present at the data lines (D5 goes high). This line goes directly to the other input of the previously mentioned AND gates.
- The outputs from the four AND gates indicate when and which of the four Octal Latches is being updated. Each output is connected to the LE (Latch Enable) pin of

[‡‡] That is, depending on the logic state of the input lines, one out of four of the output lines goes logic low, while the rest remain at logic high.
[§§] The flag D5 was added to ensure that the data to be latched is only refreshed AFTER the decoder is updated.

one of the Octal Latch chips. Thus, an Octal Latch chip is only selected for update when "selected" by the decoder and when the flag D5 goes logic low.

A summary of how such a circuit interacts with the computer during an update cycle is described below. This update cycle is repeated for as long as the control program is running:

1) Parallel port updates 8 lines with new encoder info, D5 is set low, while data info remains unchanged.
2) Decoder in the circuit updates its output, while D5 (being low) keeps the latches from updating with data from parallel port.
3) Parallel port updates 8 lines again with new data info, D5 is set high, while encoder info is unchanged.
4) Decoder sees no changes from the parallel port, and D5 (high) now allows latches to update their output with new data.

The outputs from the latches are used to "switch" on or off the MOSFETs that are used to drive the SMA actuators. Since each actuator requires approximately 1A of current to run, an IRF Z44N power MOSFET is used to drive each SMA actuator. These MOSFETs can be driven directly by standard CMOS chips. When input from the latches goes high, a voltage drop appears across the SMA wires.

LED's (Light Emitting Diodes) are placed in parallel to the actuators to indicate whether the circuitry is working or not.

Of interest to note is that since each pair of actuators has a different length from other pairs, external (power) resistors must be added to match their resistances to the same order of magnitude[***]. This is necessary to ensure that the response times of the actuators are relatively similar.

[***] Resistance of each actuator depends on its length.

Following is a flow chart representing the operation of the system, along with the schematics of the latching circuit:

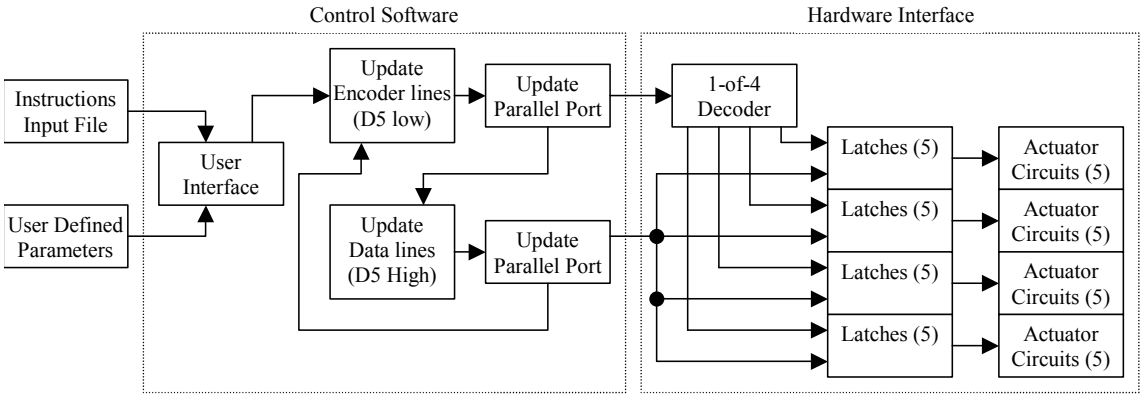

Figure 14. Control flow chart

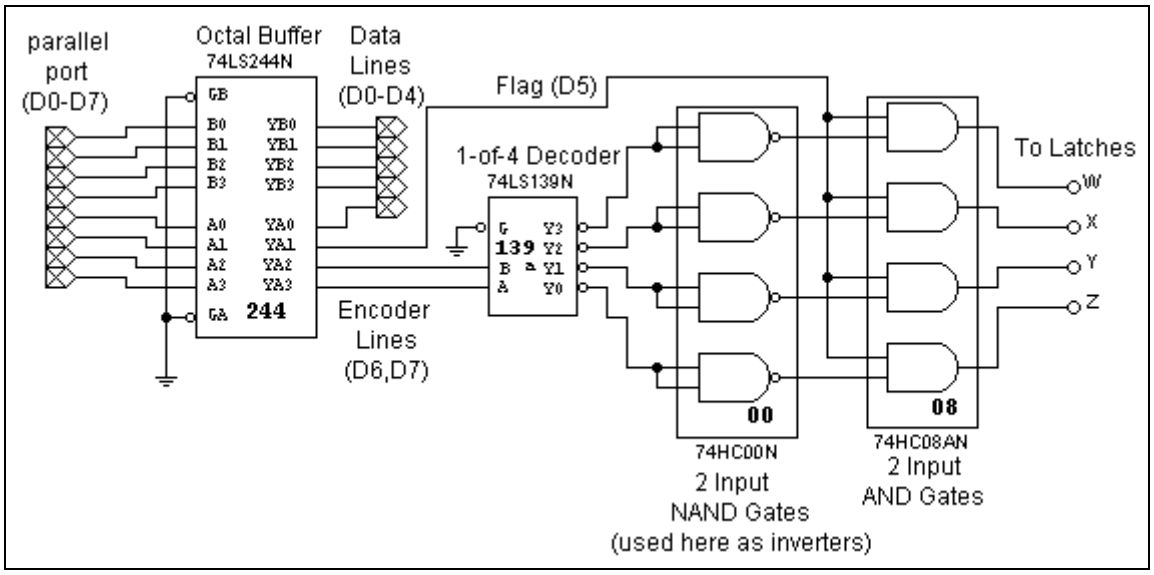

Figure 15. Latch circuit part 1

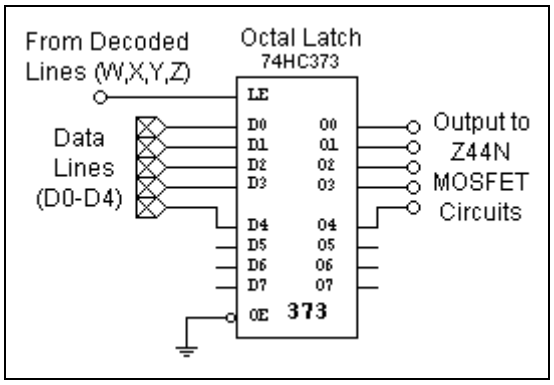

Figure 16. Latch circuit part 2

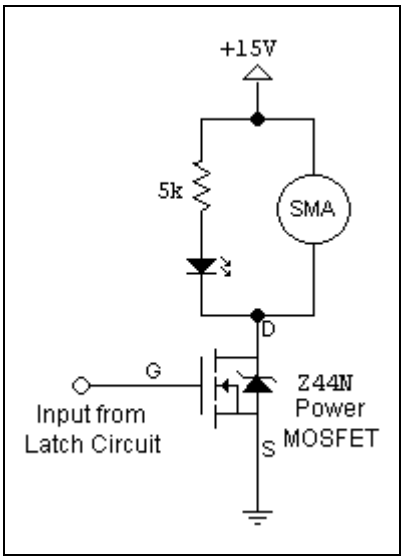

Figure 17. Latch circuit part 3

6.2 Software

LabVIEW Student Version 6i is used to control the parallel port of a laptop computer. Five lines out of twenty are updated every two clock cycles (a decoder update cycle, followed by a data update cycle). The program consists of 2 files: <controlupdate2.vi> and <controlcycle2.vi>.

The input instructions are in the form of a comma-delimited text file <*.csv> with 20 columns (one column for each actuator), consisting entirely of 1's and 0's (1 for on, 0 for off). Row 'n' of the <*.csv> file holds instructions for the time instance n*dt, where dt is a variable set by the user at the LabVIEW user interface file <controlupdate2.vi>. In the <*.csv> file, columns

1 and 2 represent the first pair of actuators, columns 3 and 4 for the second pair, and so on. The number of rows depends on the number of time points needed to define one complete cycle of the motion.

The user interface program <controlupdate2.vi> takes a user specified input file, extracts the row and column information from it, and amalgamates the data into a one-dimensional array[†††]. This array (along with the row and column information) is then passed on to the file <controlcycle2.vi>.

<controlcycle2.vi> takes the imported one-dimensional array and, for every twenty elements from the array, extracts these elements and parses this sub-array into four one-dimensional arrays each of five elements in length (corresponding to four octal latch chips, each handling five data lines). Each of these five-element arrays is subsequently passed through a sequence that first updates the two encoder lines with one of 00, 01, 10 and 11, then writes the data (five elements for five lines) to the parallel port.

Indicator lamps are placed in <controcycle2.vi> to provide a means of indicating which SMA wires should be on in real time. Screen shots from the two programs are included in the appendices.

[†††] This was done because Labview has some useful built-in functions that deal only with 1D arrays.

7 Test Apparatus

In order to conduct wet tests, the control protocols were run on a laptop at the BCRI-OEC[‡‡‡] tow tank. To support the robotic fin during testing, a simple barge was fabricated.

As the hydrodynamics of the hull is irrelevant to the determination of the thrust developed by the fin no attempt was made to design an efficient hull. Furthermore, as the simplest test to determine the maximum thrust of a propulsion system is carried out at a zero **advance velocity**[§§§] (i.e. the hull is not moving), drag would not be a factor in the thrust tests. In light of this, the main design requirements of the barge are:

- provide sufficient buoyancy to support the fin and body,
- provide sufficient stiffness against roll to prevent excessive rolling or capsize, and
- provide an accessible and adjustable mount for the fin body.

7.1 Barge Design

The barge is constructed of inexpensive polystyrene foam, plywood and scrap angle steel. To avoid the need for an opening in the centreline of the barge, a catamaran design was adopted. The catamaran design allows the fin to be suspended between the two pontoons, thus keeping the forces symmetrical and greatly simplifying the mounting of the body. For ease of calculations and manufacture, the pontoons were designed to be rectangular. The weight of the complete barge was estimated and together with the weight of the fin and hull provided the static **displacement**[****] of the test set-up. To account for the fact that the flapping of the fin would generate a rolling motion, the maximum moment that could be generated by the fin was

‡‡‡ British Columbia Research Institute Ocean Engineering Centre, located on the south campus of UBC

§§§ *(nautical)* describing the ratio of the advance of the vessel to the ideal advance of a propeller screw. In a Bollard Pole test, the advance velocity is zero, that is the boat is not moving at all. A propeller will generate its maximum thrust at an advance velocity of zero. The idea of advance velocity has been applied to the motion of a ray by Rosenberger (she uses the term **stride length**) to describe the advance of the fish through water compared to the advance of the wave on the fin.

**** *(nautical)* describing the weight of water displaced by the hull of a ship. By Achimedies' principal, this is equal to the weight of the vessel itself. (Course Notes for Mech 341, Jon Mikkelsen, UBC)

calculated and the resultant additional force on the reacting pontoon was determined. This force was added to the static displacement to determine the worst-case dynamic displacement of the pontoon. From the estimated dynamic displacement, the maximum required submerged volume of the pontoons were calculated. The length of the hull was specified to be 610 mm (24-inches), and the cross-sectional area of the submerged pontoon was chosen to be square. To provide a factor of safety, the maximum required submerged volume was doubled to provide the **scantlings**[††††] for the catamaran hulls.

7.2 Construction

The two pontoon hulls were constructed by gluing a 2-inch thick by 6-inch wide strip of expanded Styrofoam to either side of two 7 5/8-inch wide, ¼-inch thick plywood strips. Both foam and plywood strips were 24-inches long. Exterior grade glue designed to attach foam to wood was used to laminate the strips. As there was some concern that some of the smaller beads from the foam would break off in the tow-tank, the pontoons were covered with sailcloth attached with double-sided sail-makers tape. A diagram of pontoons is shown below in Figure 18.

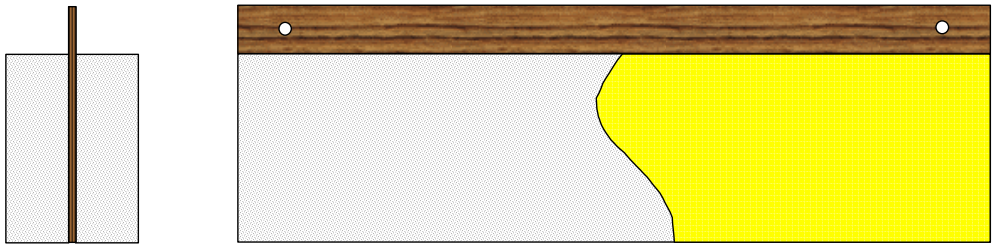

Figure 18. Pontoon diagram

The two pontoons were connected using steel angles (Handy© shelving material) at the bow and stern of the barge. Each crossbeam supported a pair of vertical angles, between which the body of the fin was clamped on the centreline of the vessel.

[††††] *(nautical)* describes the dimensions and sizes of all structural parts of a vessel (Building Small Boats, Greg Rössel, 1998 WoodenBoat Publications Brooklin Main)

7.3 Drag Estimation

Both the barge hulls and the power cable were sources of drag acting on the robotic fin.

The best way to determine the drag of a hull shape is to conduct an empirical test on the vessel, or a model of the vessel. A determination of the drag of the barge was not made during the testing for two reasons. Firstly, as stated above, the intention of the barge was to provide a platform on which to conduct static thrust tests. Secondly, in free-swimming tests (the only tests that were actually performed), the vessel achieved no discernable movement even though a very small nudge could be seen to set the fin in motion, and so the drag of the vessel was considered to be negligible.

The primary restraint acting on the vessel was the spring constant of the connecting cable to the fin. Straightening the cable and floating a length behind the barge and fin minimized the effect of this.

The force required to move the barge, even accounting for the attached cable and boxy hulls was quite low, on the order of a few newtons, but could not be quantified in the tests conducted.

8 Testing

Testing on the Robo-Ray was conducted in the towing tank located at the British Columbia Research Institute Ocean Engineering Centre at UBC.

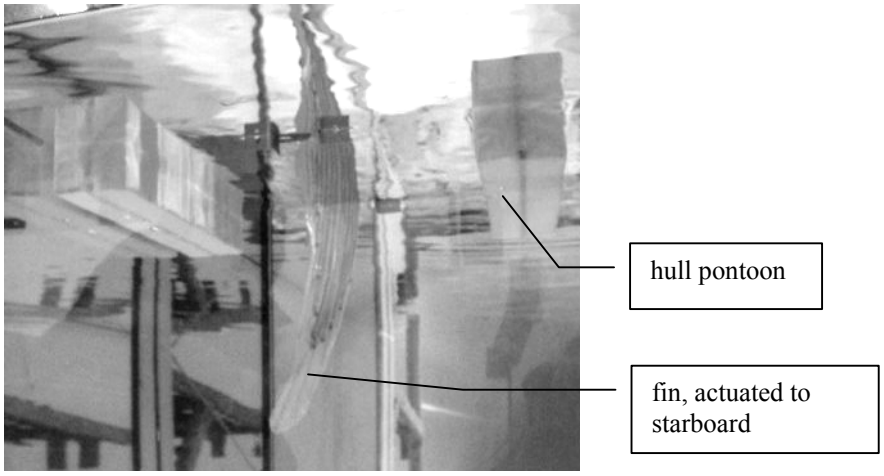

Figure 19. Underwater photo of the robot ray at the BCRI OEC

To produce a symmetric stroke, before beginning the testing sequences, the actuator lines must be tensioned or "tuned" to produce the same forces in either direction.

Tuning the Lines

Tuning of the actuator lines was carried out in two stages. The first tuning step was carried out in air. In this step, the lines on one side were actuated continuously, and the lines were tensioned to achieve the desired fin amplitude and fin shape. The amplitude of the fin was measured at the distal tip, and adjusted by tuning lines 10 and 12 (the longest wires). The other actuator lines were then adjusted to achieve a fair membrane shape. The lines on the tuned side were then allowed to cool, and then the process was repeated for the other side. Once both sides had been tuned, the process was repeated on each side to adjust for the effects of tuning the other side. Care has to be taken not to over-tension the wire, or too much force will be needed to overcome the restoring force from re-stretching the relaxing wire.

The second round of tuning was similar to the first step, but was carried out with the fin mounted on the barge and in the water. For this step, the fin was slowly oscillated (~5 seconds per side) with one whole side (or a section of a side) on at a time. The objective of this tuning was to ensure symmetrical amplitudes, rather than absolute amplitudes. Some fine-tuning was also carried out during the undulation tests, to try and improve the fin shape or relative batten positions.

Testing Procedure

Due to the short time available for testing, qualitative observations were made with a variety of input instructions to the fin. The observations from the testing are summarized below in Table 2. The step time refers to the length of time each line (step) of the <*.csv> file is executed for. The step sequence is the repeating input pattern that defines the waveform to be placed on the fin membrane. One such test pattern is shown graphically in the appendices. Note that there are 16 values in the step sequence, but only 10 elements on the fin. This is due to the observation by Rosenberger et al. that the species *G. micrura* has approximately 60% of a full waveform on its fin while swimming. The input voltage is the voltage measured at the power supply. There is approximately 14-ohms resistance across each wire, and 1-ohm resistance in the power cable.

Table 2. Test observations

Step Time	Step Sequence U=up, O=off, D=down	Input Voltage	Observations
1 sec.	4U, 4O, 4D, 4O	7 VDC	No discernable forward movement
1 sec.		10 VDC	No discernable forward movement
0.5 sec.		10 VDC	Smoother flapping of fin, no forward movement
0.25 sec.		15 VDC	No discernable forward movement
0.25 sec.	3U, 5O, 3D, 5O	15 VDC	Best movement, possibly forward movement on first beat of fin
0.25 sec.	2U, 6O, 2D, 6O	15 VDC	No discernable forward movement

In all cases, the fin responded properly to the control input.

The only actuation where forward motion was observed was the fifth set of observations. Unfortunately, two factors prevented the observation of motion from being more definite. Firstly, and most importantly, after the first or second cycling of the fin, the fin failed to invert properly. Secondly, the stiffness of the attached power cord transmitted a significant amount of spring force to the model, impeding forward motion. However, the indication of motion would suggest this combination as a logical starting point for future work.

9 Results

The final product of this project is an articulated two-dimensional surface. Oscillation and undulation are possible with this physical model, although severely limited by difficulties with maintaining the correct orientation between the muscle and batten elements of the fin structure. A solution has been identified that may resolve this issue, but is however not possible to implement within the time remaining for this project. We have also developed a two-element prototype of the fin, which can be used to test alterations to the fin design before applying the modifications to the 11-element fin. To augment the physical model, a detailed mathematical model of the fin motion has been developed to describe the motion of the *G. micrura*, and therefore the desired motion of the robotic fin.

While the ultimate goal of useful propulsion was not achieved, an excellent foundation has been laid for further work in the development of rajiform propulsion. Beyond the physical model itself, the control circuitry, controlling computer program and the mathematical models of the motion will greatly aid in the further development of this mode of propulsion.

10 Conclusions

While Robo-Ray has not successfully produced quantifiable forward motion yet, it would be a good idea to continue to explore this design to the limits of modifications recommended herein.

Further research into rajiform motion may produce a viable propulsion system that is elegantly-suited to submersible vehicles. This project can lay the groundwork for possible future projects to measure the propulsion by testing the fin quantitatively in the tow tank, to optimize the motion and the shape of the fin, and combine propulsion and steering functions in the control algorithm.

11 Recommendations

As a result of our work on this project, we are making the following recommendations for continuing work:

1. Mechanical design of fin: Solutions to the following problems should be addressed in an integrated manner:
    a. Improve the design of the SMA wire attachment to bone to maintain separation and facilitate proper fin inversion. The failure to obtain proper fin inversion was likely the greatest impediment to generating thrust from the fin.
    b. Revisit the batten design. Rays have segmented pectoral "bones". This would reduce the stiffness of the fin (and thus the force required to bend the fin) and fatigue on the batten material.
    c. Devise a method of covering fin to present a smooth outer surface. The "open architecture" of the fin constructed for this project presents an undesirable hydrodynamic surface; this will need to be rectified to obtain the best propulsion possible from the fin.
2. Application of the mathematical model to robot motion: Due to time constraints, the mathematical models of the undulatory and oscillatory swimming motion were not adequately applied in a control algorithm. In conjunction with recommendation #3, the mathematical model should be applied to generate a more complete control program.
3. Control of the actuating muscles: Further work needs to be done on controlling the SMA material if it is to be used effectively as an actuator in this application.
    a. Mathematical models generated during this project should be applied to the control.

b. Force, position and temperature sensors should be added to the fin elements to allow a feedback control strategy.

c. Further work should be conducted with respect to characterizing the response of the SMA material in the thermal and mechanical load conditions experienced in this application.

d. The control strategy should manage the power supplied to the wires so that the desired response is obtained and the wire is not overheated. Power regulation through pulse width modulation would be one way of achieving this control.

4. Asymmetry of fin and swimming stroke: Studies on rays and our mathematical models of *G. micrura* show that the swimming stroke and wing shape of rays are asymmetric. More investigation into the effects of the asymmetry on force generation should be undertaken. Consideration should then be given to re-configuring the control algorithms and wing design to reflect this asymmetry.

12 Acknowledgements

This project made use of many resources available at UBC. The team would like to thank the following people for their assistance:

- Dr. Ahlborn – for help understanding the theory
- Al Cheuck – for assistance and support with the electronics
- Harold Davis – for general support, loan of the digital camera and Lambda power supply
- Paul Killeen of Ullman Sails Vancouver – for the sailcloth and tape donation
- Jon Mikkelsen – for design advice
- Gerry Stensgardd and BCRI – for tow tank access

13 References

1. Hubbard, Richard L. *Buoyancy, fins and swimming*. Hubbard's Fish Anatomy. http://www.nova.edu/~rlh/text/fins/fins.html. (Graduate Candidate, Nova SE University)
2. Maslin, Paul. "Biology 261 Ichthyology." Course Notes. CaSU. last updated Feb.6, 1996. http://www.csuchico.edu/~pmaslin/ichthy/loco2.html
3. Rosenberger, L.J. *Pectoral fin locomotion in batoid fishes: undulation versus oscillation*. Journal of Experimental Biology 204 (2001) pp379-394.
4. Rosenberger, L.J. (2001) p391.
5. Hamlett, W.C. Sharks, Skates, and Rays : the Biology of Elasmobranch Fishes. John Hopkins University (1999). p135.

Other General References

Rosenberger, L. J., Westneat, M.W. *Functional morphology of undulatory pectoral fin locomotion in the stingray Tainiura Lymma (Chondrichthyes: Dasyatidae)*. Journal of Experimental Biology 202 (1999) pp3523-3539.

McHenry, M. J. et al. *Mechanical control of swimming speed : stiffness and axial wave form in undulating fish models*. Journal of Experimental Biology 198 (1995) pp2293-2305.

Webb, P.W. Hydrodynamics and Energetics of Fish Propulsion. Department of Environment, Fisheries and Marine Services. Nanaimo, BC, Canada (1975).

Shuttleworth, T.J. (Ed). Physiology of Elasmobranch Fishes. Springer-Verlag Berlin. Heidelberg, Germany (1988).

Aleev, Y.G. Function and Gross Morphology in Fish. Trans. Keter Press. Jerusalum (1969).

Appendix A Modelled Motion for *G. micrura*

The following graphs, generated in Matlab, show the sequence of sail edge positions. The mathematical model (from section 4.2) is based on photographs from Rosenberger [3] at 0 s, 0.183 s, 0.366 s, 0.549 s and 0.749 s. In each case, the crossed line is the current position, the dashed lines are the previous positions, and the dots are the initial (t = 0 s) position of the fin edge.

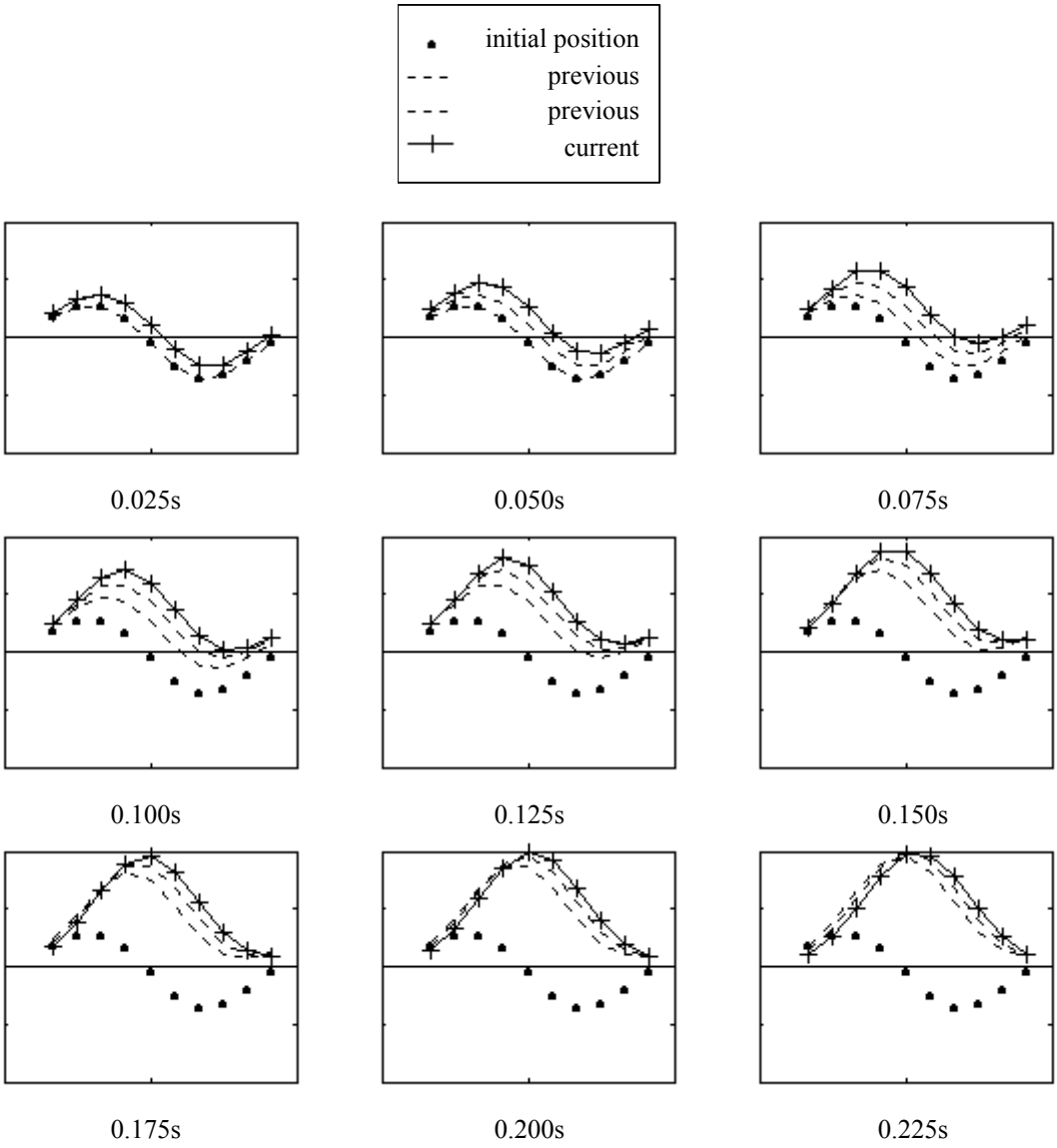

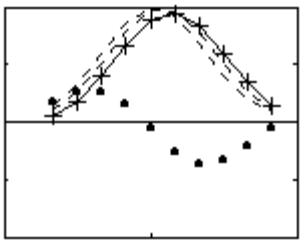

0.250s

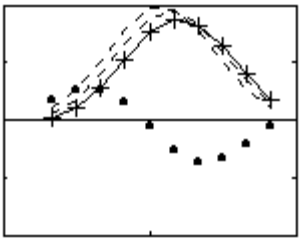

0.275s

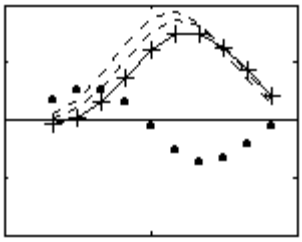

0.300s

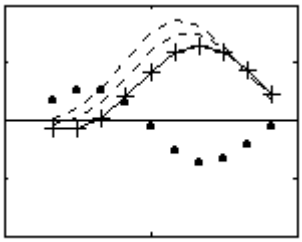

0.325s

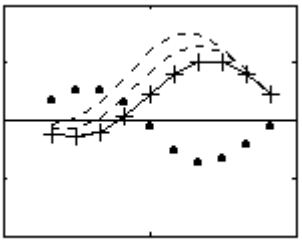

0.350s

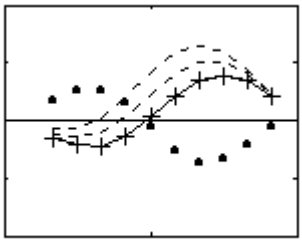

0.375s

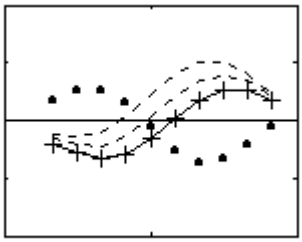

0.400s

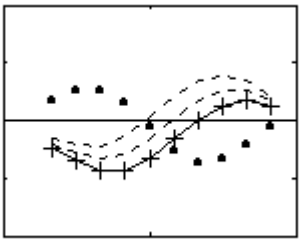

0.425s

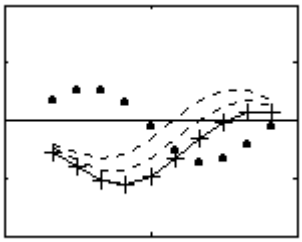

0.450s

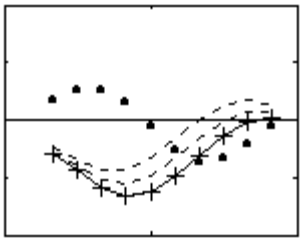

0.475s

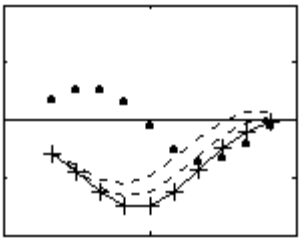

0.500s

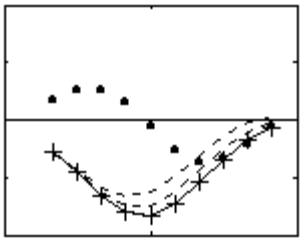

0.525s

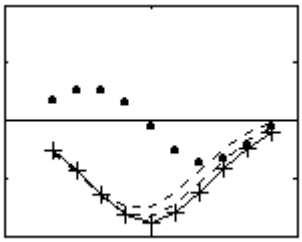

0.550s

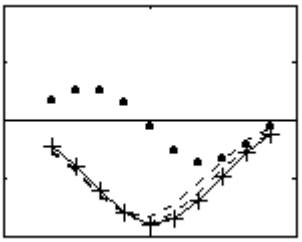

0.575s

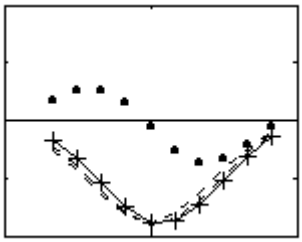

0.600s

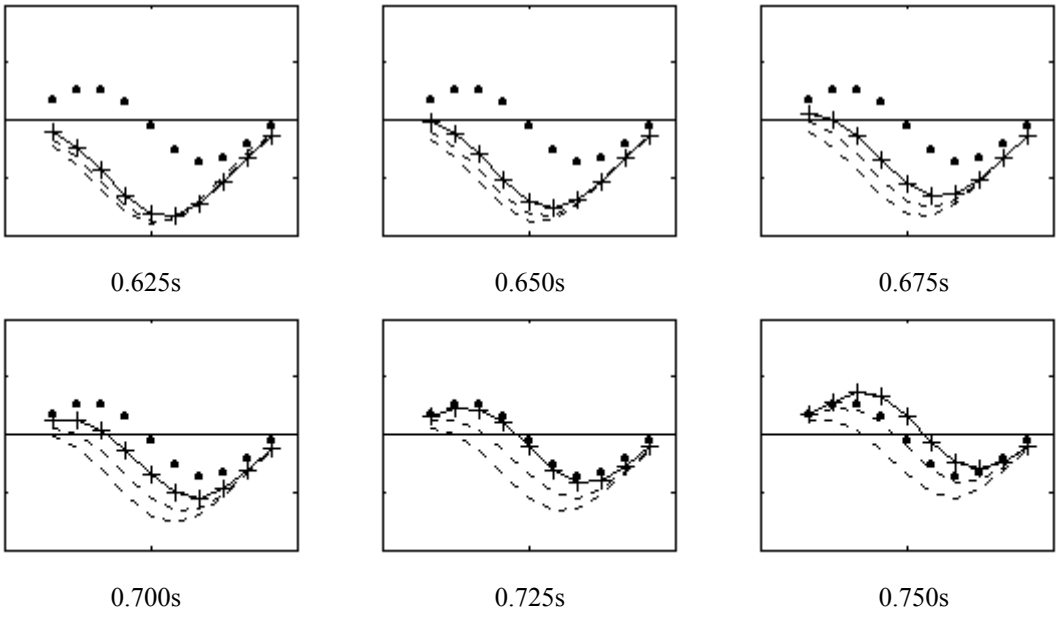

Figure 20. Consecutive fin motion steps

Appendix B Mechanical Drawings

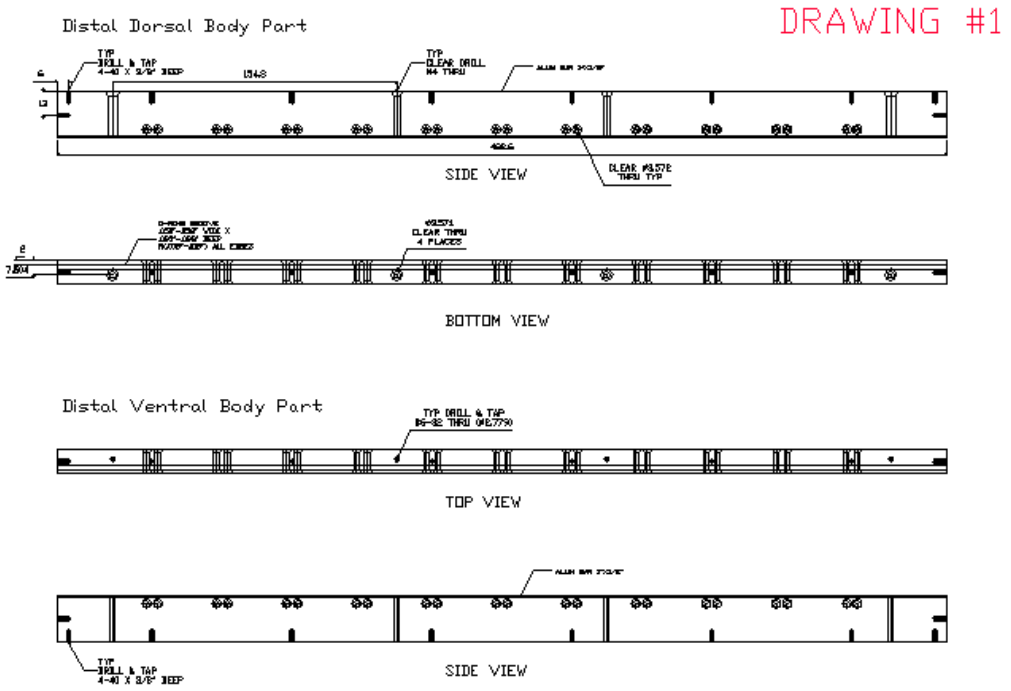

Figure 21. Distal body parts

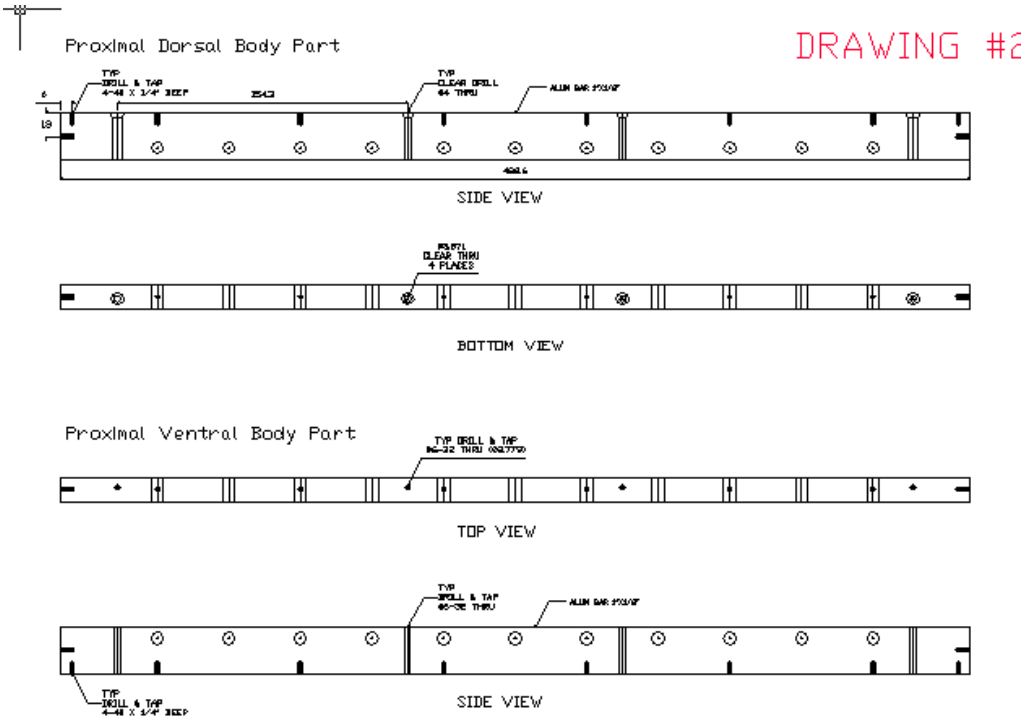

Figure 22. Proximal body parts

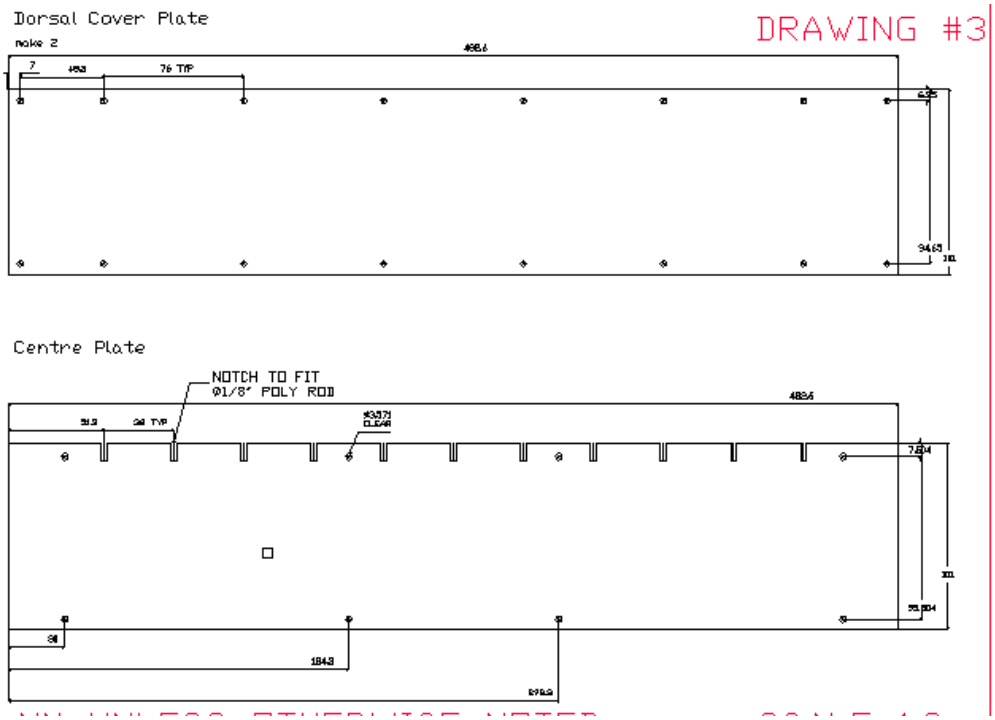

Figure 23. Cover plates

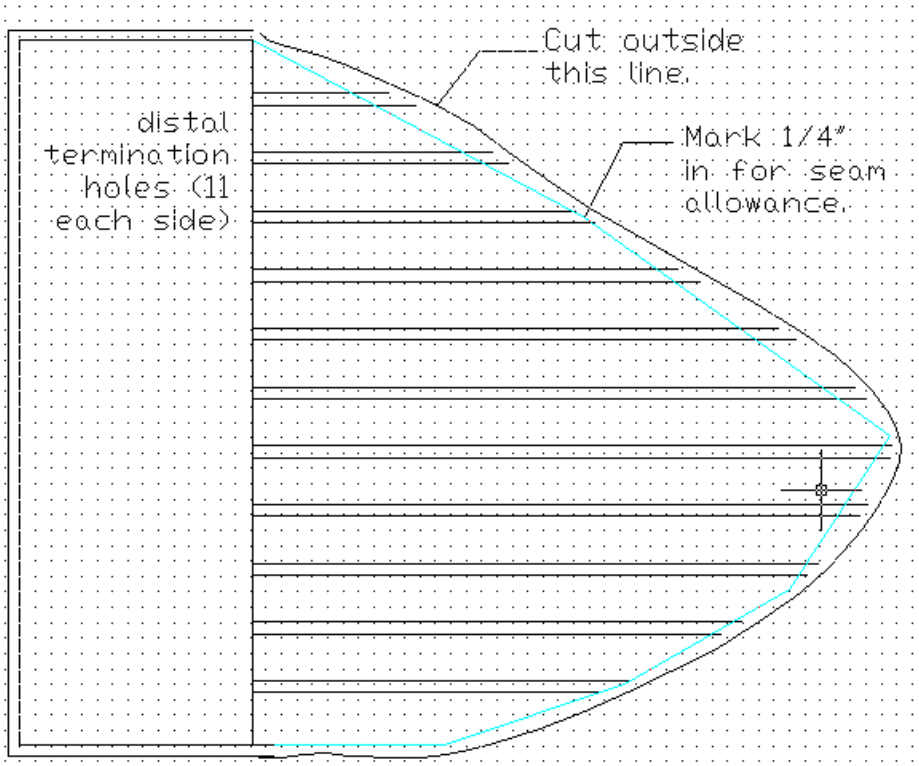

Figure 24. Sail cloth pattern

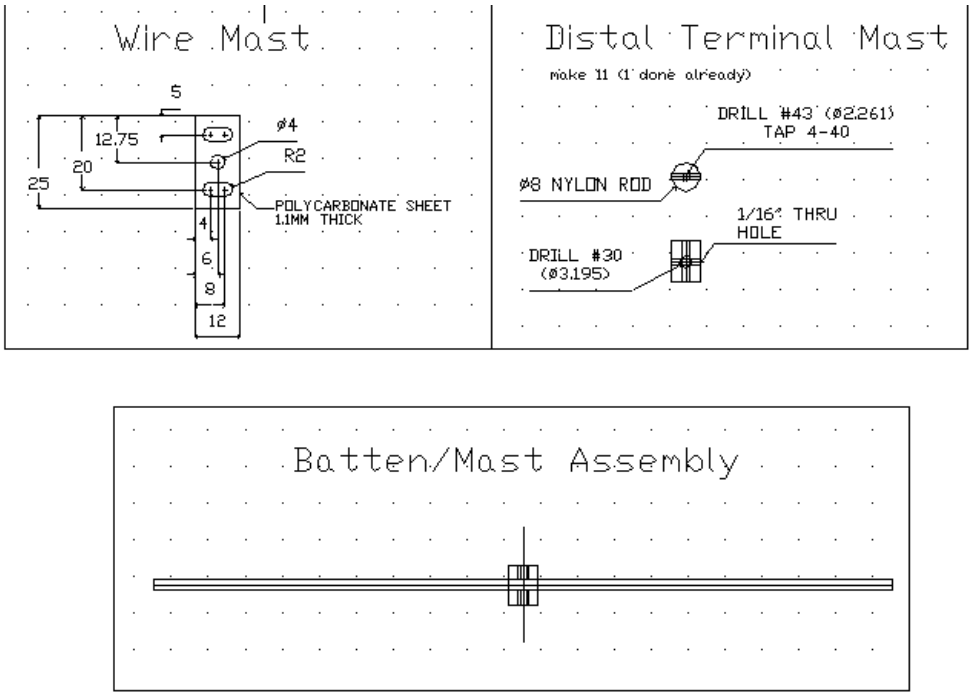

Figure 25. Small bits

Appendix C Prototype Testing Circuit

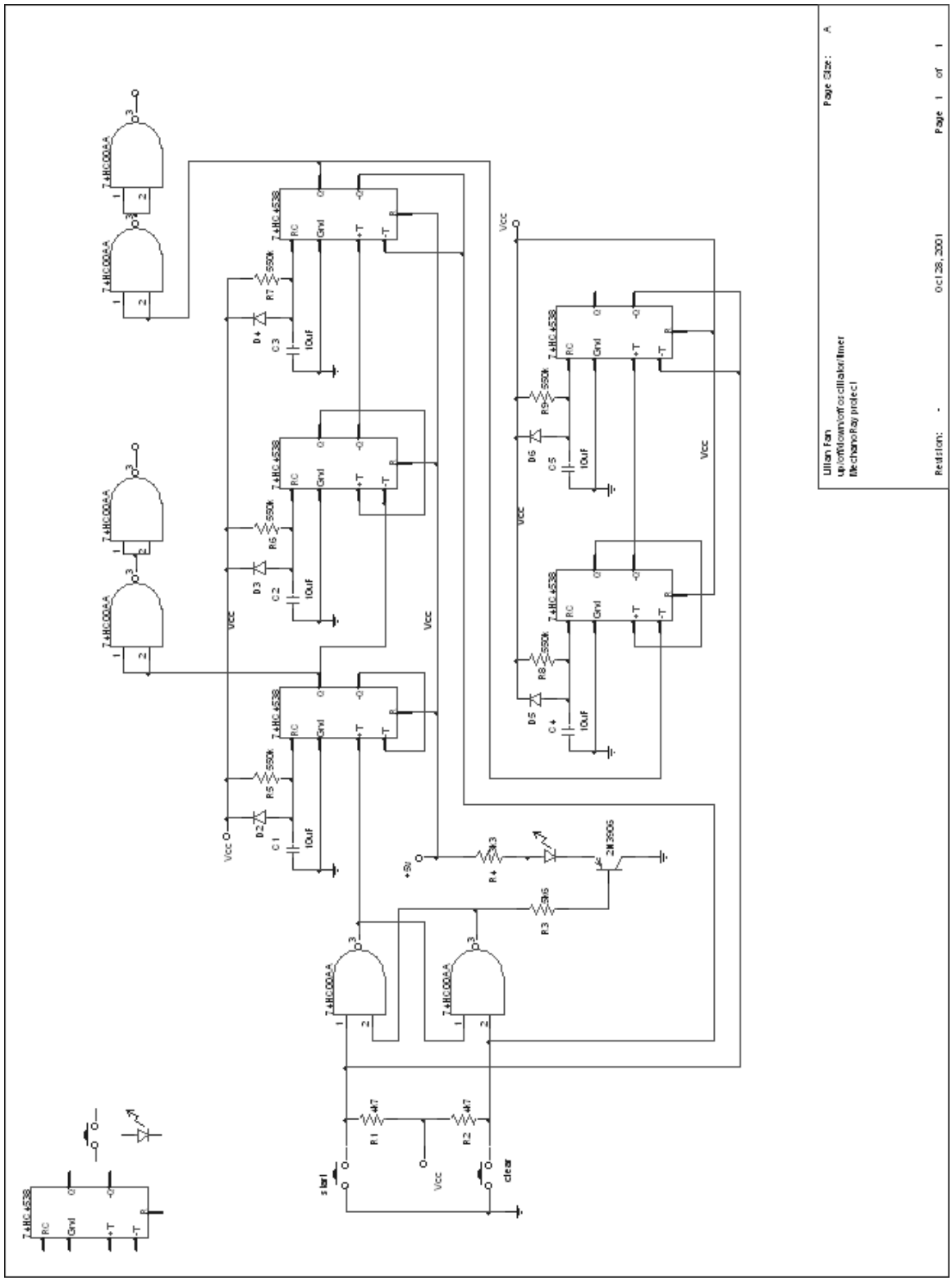

Figure 26. Prototype testing circuit diagram

Appendix D LabVIEW Screenshots

The following figures show the LabVIEW interfaces designed for this project (see section 6.2 for details).

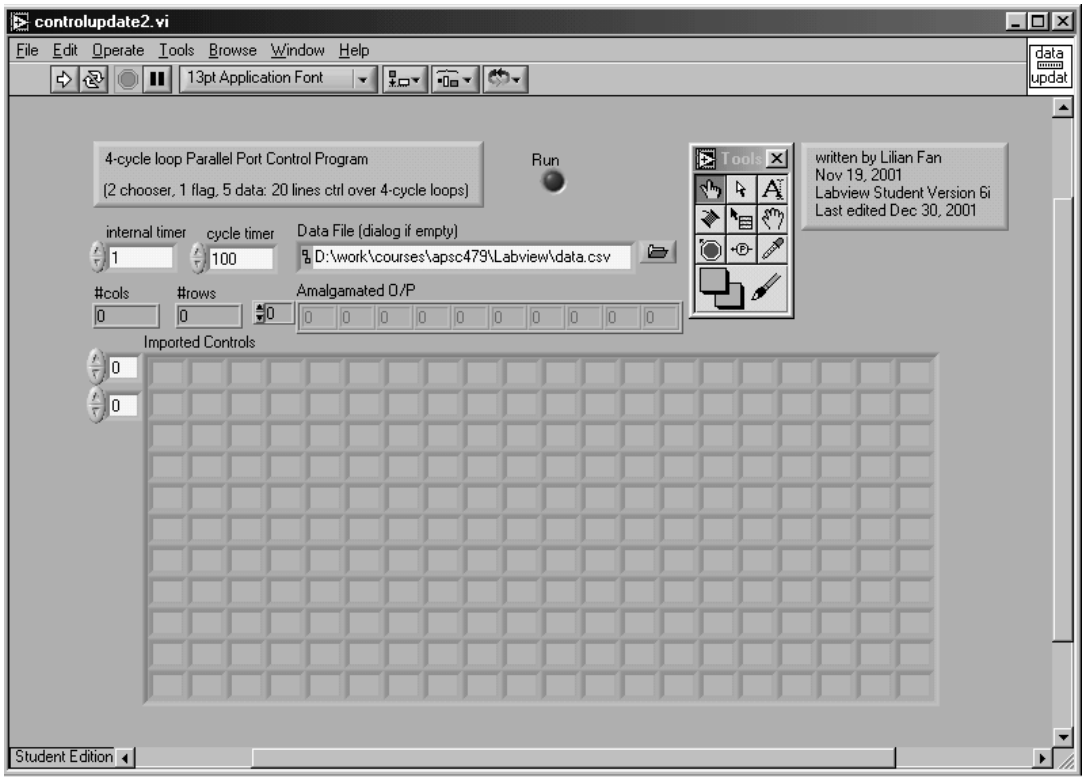

Figure 27. Screenshot of Labview front panel for <controlupdate2.vi>

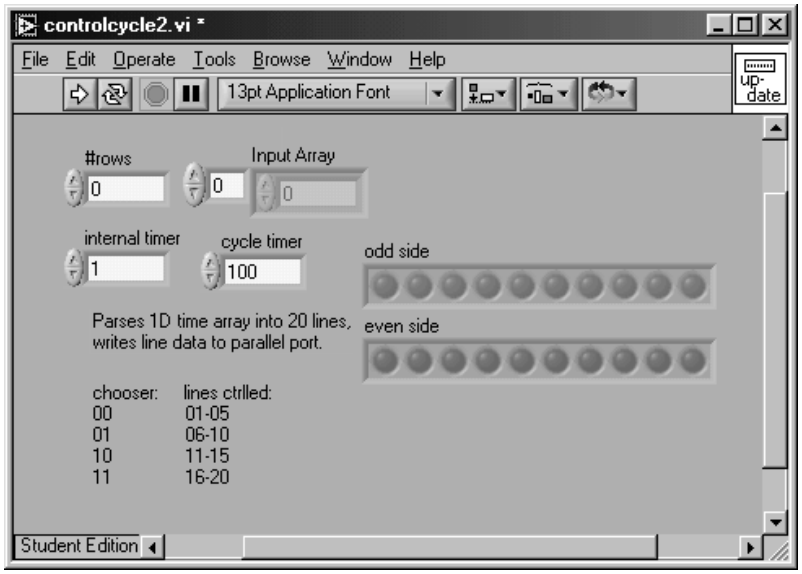

Figure 28. Screenshot of LabVIEW front panel for <controlcycle2.vi>

Appendix E Matlab Modeling Files

The following Matlab scripts were used to model the motion of the *G. micrura* fin edge.

```
%%%%%%%%%%%%%%%%%%%%%%%%%%%%%%%%%%%%%%%%%%%%%%%%%%%%%%%%%%%%%%%%%%%%%%%%%%%%
%file: targettest.m                                                            %
%%%%%%%%%%%%%%%%%%%%%%%%%%%%%%%%%%%%%%%%%%%%%%%%%%%%%%%%%%%%%%%%%%%%%%%%%%%%

%testing target shape
clear all;

t=0:0.0625:.75;
lines=1:1:10;
x=(lines+1)/(length(lines)+2);  %11 bones, the first one not activated

for j=1:length(t)
linex=[0 1];
liney=[0 0];
plot(linex,liney,'k-');
axis([0 1 -.4 .4]);
%axis([0 1 -.3 .3]);
set(gca,'yTickLabel',{''});
set(gca,'xTickLabel',{''});
hold on;

y=target(0,lines);
plot(x,y,'k.');
y=target(t(j-2),lines);
plot(x,y,'k:');
y=target(t(j-1),lines);
plot(x,y,'k:');
y=target(t(j),lines);
plot(x,y,'k+-');
hold off;
end
```

```
%%%%%%%%%%%%%%%%%%%%%%%%%%%%%%%%%%%%%%%%%%%%%%%%%%%%%%%%%%%%%%%%%%%%%%%%%%%%
%file: target.m                                                                 %
%%%%%%%%%%%%%%%%%%%%%%%%%%%%%%%%%%%%%%%%%%%%%%%%%%%%%%%%%%%%%%%%%%%%%%%%%%%%

function [R]=target(t,lines)
% ctrl=2lines
% initialize line dependant constants
x=(lines+1)/(length(lines)+2);  %11 bones, the first one not activated

k0=0.2;

%following from fitted parameters

FinShape=-69.9975*x.^6+207.078*x.^5-230.749*x.^4+117.086*x.^3-
27.7372*x.^2+4.41192*x-0.00789179;
lambda=1.1027+0.21982*sin(8.4063*t+3.6355);
phi=-0.033771+1.4071*t;
OscComp=0.1+1.25*sin(8.5*t);    %this was manually fitted.  not very
good.

R=k0*FinShape.*(sin((2*pi/lambda)*(x-phi))+OscComp);
%R=k0*FinShape.*(sin((2*pi/lambda)*(x-phi)));
%R=k0*FinShape*OscComp;
```

Appendix F IGOR Curve Fitting File

The following IGOR Pro file was used for fitting the data curves to Gaussians.

```
#pragma rtGlobals=1           // Use modern global access method.

Function MultiSine (coeffs, xposn)

//declare variables and waves
      wave coeffs;
      variable xposn
      variable k0,k1,k2,k3,S,R

//input parameters

      k0=coeffs[0]                  // env amplitude
      k1=coeffs[1]                  // moving freq w
      k2=coeffs[2]                  // moving phase chg
      k3=coeffs[3]                  // const

//fin shape
S=-69.9975*x^6+207.078*x^5-230.749*x^4+117.086*x^3-
27.7372*x^2+4.41192*x-0.00789179

//superimposed

R=k0*sin(pi*x)*(sin((2*pi/k1)*(x-k2))+k3)

//return statement
      return R

End
```

Appendix G Test Inputs

The following sequence of plots represents the test input.

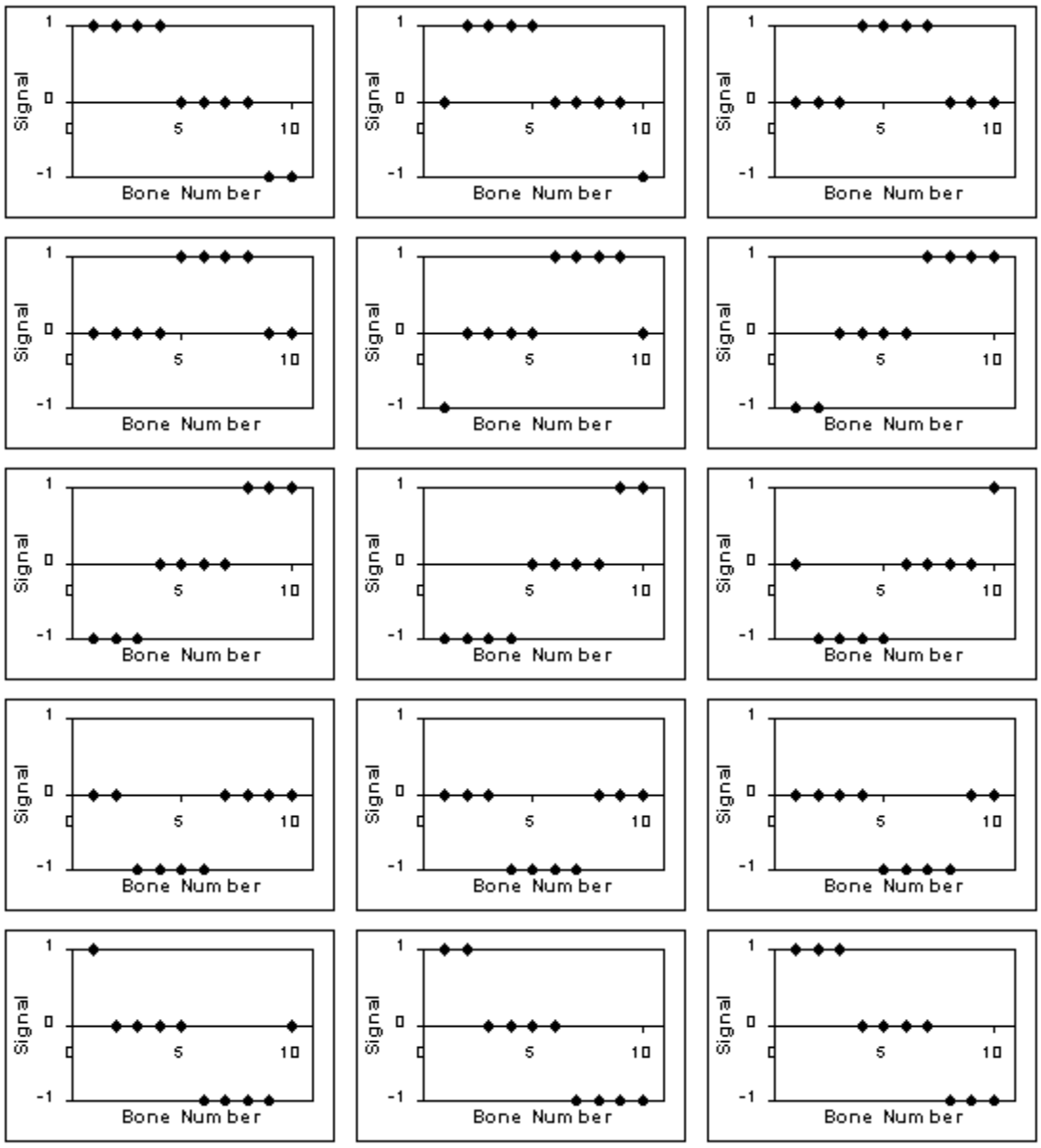

Figure 29. Undulatory input signals

Appendix H Project Self-Evaluation

The team is quite successful in the sense that all members of the group were able to work together to coordinate and divide up tasks for this relatively adventurous undertaking. The primary obstacles impeding the progress of the project, as it turns out, were issues of SMA wire attachments, as well as general time management.

Overall, the group considers the project to be relatively successful in the sense that the objectives our group set out to meet have been met – to build a controllable 2D surface capable of emulating the undulatory and oscillatory swimming modes of rays. Despite the fact that the fin is not yet propelling itself in water, test results from both the fin and the prototype exhibit evidence that it is possible to achieve much finer control of the fin given time.

The group feels that the project can be improved and intends to continue work on it so that it will be ready for the Western Engineering Conference & Competition next week. The project will also be presented at the next SNAME[‡‡‡‡] student presentation meeting.

[‡‡‡‡] Society of Naval Architects and Marine Engineers